Fast Calibration of Speed-of-Sound using Temperature Prior in Whole-Body Small Animal Optoacoustic Imaging

Subhamoy Mandal^{a,b}, Elena Nasonova^c, X Luís Deán-Ben^a and Daniel Razansky^{a,b}
^aInstitute for Biological and Medical Imaging, Helmholtz Zentrum München, Germany
^bTechnische Universität München, Munich, Germany
^ciThera Medical GmbH,Munich, Germany

ABSTRACT

The speed of sound (SoS) in the imaged sample and in the coupling medium is an important parameter in optoacoustic tomography that must be specified in order to accurately restore maps of local optical absorbance. In this work, several hybrid focusing functions are described that successfully determine the most suitable SoS based on post-reconstruction images. The SoS in the coupling medium (water) can be determined from temperature readings. Thereby, this value is suggested to be used as an initial guess for faster SoS calibration in the reconstruction of tissues having a different SoS than water.

Keywords: Optoacoustic tomography, photoacoustic tomography, image analysis, speed of sound variations, image reconstruction

1. INTRODUCTION

Optoacoustic tomography (OAT) enables high resolution visualization of optical contrast, through its hybrid nature of optical excitation and acoustic detection. The technology has emerged as a versatile tool for biological imaging, owing to its optical contrast and high (diffraction-limited) spatial resolution associated with low-scattering ultrasound waves, as opposed to photon propagation.^{1,2} The instrumentation of the majority currently used optoacoustic scanners incorporates a coupling medium (typically water) as an interface between the scanning objects and ultrasound detectors.³ The temperature of the medium is generally kept uniform and constant during the entire scanning period, where stirring and external heating is commonly applied. However, it is observed that drifts in the temperature over time can cause aberrations in image quality.⁴ We have earlier shown that focusing algorithms can be used to correct for these temporal variations in temperature profile, and the image quality can be enhanced by factoring temperature information during reconstruction and postprocessing of OAT images.⁵ Accurate calibration of reconstruction parameters plays a vital role for optimizing the resolution and contrast as well as associated quality measures of optoacoustic tomographic images, where the speed of sound (SoS) is an important parameter. Commonly, a constant value of the SoS in biological tissues is assumed for tomographic reconstructions. However, spatial variations of the SoS, attenuation and other acoustic properties of the propagation medium affect the collected optoacoustic signals and therefore must be correctly accounted for in the reconstruction procedure. The SoS in the medium (and the tissue) is a function of the temperature, thus the SoS calibration can be directly linked with variations in temperature. This allows us to use of a priori temperature information (of the medium) not only as a parameter for correction of temporal fluctuations of temperature^{4,5} but also as an initial guess for fast calibration of SoS for reconstruction. In this work, several hybrid focus functions are described that present higher sensitivity and success rate in determining the best matching SoS compared to state-of-the-art approaches. The hybrid autofocusing measures incorporate key improvements, viz. edge detection or diffusion, which not only enhance the focusing performance but also makes them more suitable for reconstructing realistic tomographic images acquired from small animals.⁷ Furthermore, the a-priori determined SoS from temperature reading in the coupling medium (water) is used as an initial guess for a fast calibration of the SoS in the reconstruction. Continuous monitoring of temperature is shown to significantly increase the convergence speed of the methods and also aid in correcting for temporal variations in SoS, which can degrade image quality.⁵

Further author information: (Send correspondence to Subhamoy Mandal) Subhamoy Mandal.: E-mail: s.mandal@tum.de, Daniel Razansky.:E-mail: dr@tum.de IBMI, Helmholtz Zentrum München, Ingolstädter Landstraße 1, 85764 Neuherberg, Germany.

Photons Plus Ultrasound: Imaging and Sensing 2015, edited by Alexander A. Oraevsky, Lihong V. Wang Proc. of SPIE Vol. 9323, 93232Q · © 2015 SPIE · CCC code: 1605-7422/15/\$18 doi: 10.1117/12.2079424

Proc. of SPIE Vol. 9323 93232Q-1

2. OPTIMAL CALIBRATION OF SPEED OF SOUND

The most frequently used optoacoustic reconstruction algorithms use approximated inversion formulae by assuming that the imaged sample corresponds to a uniform non attenuating acoustic material perfectly matched to the coupling medium (water).⁸⁻¹² Further, it is also assumed that the temperature of the water bath (and the object) is kept constant over the period of experimentation. While these assumptions are sometimes valid to model actual soft tissues, the tomographic reconstructions obtained with such algorithms are generally affected by reduced resolution, quantification errors and other artefacts. We analyzed the efficacy of iterative algorithms which reconstructs selected frames at different SoS and computes the sharpness and edge information of the reconstructed images to find out the most suitable SoS.^{13,14} Assuming that the best focusing performance is achieved when the SoS is closest to its actual value, the most suitable speed can be identified for a given dataset. Given the fact that change of temperature is also a function of time, this process was re-iterated over a short interval, yielding a fair estimate of instantaneous SOS for real-time reconstruction. The workflow for a typical SoS calibration procedure is depicted in figure 1, the best match for the SOS is achieved when the final reconstructed image is in sharp focus, the temperature prior defines the search space for fitting SoS.

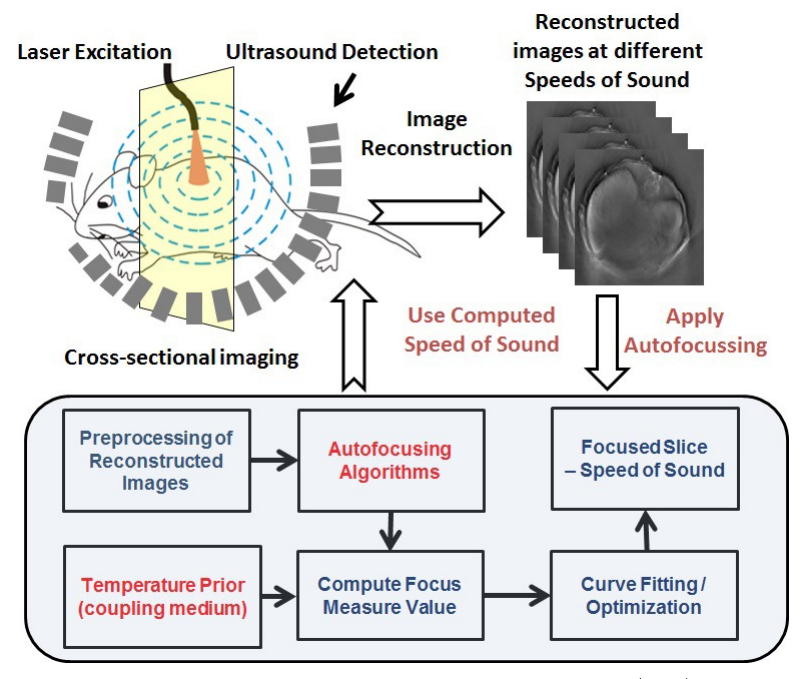


Figure 1: The algorithmic workflow for self-calibration of speed of sound (SoS) based of post reconstruction optoacoustic images, the temperature of the coupling medium is used as a prior to initiate the search for suitable SoS. The value of SoS used for reconstructing the most focused image yields the calibrated speed.

2.1 Focus Measures

In this work, we describe a group of hybrid metrics which integrates image filtering, autofocusing and image reconstruction. For comparison, we also use several other traditional focus measures. For statistical evaluation, focus metrics were calculated on the interval from 1460 to 1580 m/s, corresponding to a typical range of SoS in water and soft tissues, with step size of 1 m/s, processed with smoothing Savitzky-Golay denoising filter, and normalized to unity prior to display.⁷ The proposed algorithms tested are presented are the following:

Normalized sum of edge pixels (Edge+Sum)

The method computes the sum of pixels corresponding to strong edges, subsequently normalized by the total number of pixels in the image. The Sobel approximation to the derivative is used as edge detection algorithm. The objective of the method is to minimize the influence of thin circles and 'crossing-arcs' artifacts typically

present in unfocused cross-sectional optoacoustic images. The method then aims at maximizing clearly defined edges, i.e., it represents, to some extent, an opposite approach to the traditional camera focusing. The focus measure is then expressed as

$$F_{ES} = \frac{1}{N} \sum_{x,y} e(x,y),\tag{1}$$

$$e(x,y) = \begin{cases} 1 & \text{if } g(x,y) \ge \text{threshold} \\ 0 & \text{otherwise} \end{cases}$$
 (2)

$$g(x,y) = \sqrt{[G * f(x,y)^2] + [(G^T) * f(x,y)]^2}, \quad \text{N being the number of pixels in the image}$$
 (3)

f(x,y) is a function of two variable that represents the gray scale intensity in the cross-sectional OAT image and G denotes the Sobel operator.¹⁵

Normalized variance of the image gradient magnitude using Sobel operator (Sobel+Var)

As an improvement to the normalized variance of the image, the variance of the gradient magnitude obtained by convolution with the Sobel operator is computed instead. This metric is a combination of statistics-based and derivative-based algorithms, leading to an enhanced performance in optoacoustic images. The focus measure is expressed as

$$F_{SV} = -\frac{1}{N\mu} \sum_{x,y} (g(x,y) - \mu)^2, \quad \mu = \text{mean of } g(x,y)$$
 (4)

Anisotropic diffusion enhanced energy of image gradient using consistent gradient operator (Ad-CG)

Ad-CG is a hybrid methodology based on a combination of anisotropic diffusion ¹⁷ and consistent gradient (CG) operator. The diffusion process removes noise and intensity fluctuations - and reduces the ripples in focus measure as a function of the SoS. A Consistent Gradient (CG) operator thereafter computes the energy of the image gradient to calculate the focus measure scores. The method provides more stable performance under varying conditions by ensuring the exactness of gradient direction in a local one-dimensional pattern irrespective of orientation, spectral composition, and sub-pixel translation.

The focus measure including all intermediate steps can be expressed in a form:

$$F_{ADCG} = -\frac{1}{N} \sum_{x,y} w.I_H + (1-w).I_V$$
 (5)

where N is the total number of image pixels and w is an additional factor allowing for flexibility in assigning more weight to horizontal I_H or vertical I_V derivative approximations, which can be further be expressed as:

$$I_H = CG * I_{AD}; I_V = CG^T * I_{AD}$$

$$\tag{6}$$

 I_{AD} is the optoacoustic image after anisotropic diffusion filtering and CG being the 5x5 consistent gradient operator. ¹⁸

2.2 Temperature Priors for fast self-calibration

The temperature of the coupling medium is constantly monitored by a thermocouple capable of tracking 0.1° C changes in the water temperature. Any changes over 0.5° C is sampled and factors for image correction and re-calibration purposes. Ideally, a uniform temperature of 34° C is attempted to be maintained, for which the SoS in water is 1510 m/s. Using this as a priori information, the optimization is done in a range of $\pm 25 \text{ m/s}$ with respect to SoS in water. This drastically reduces the total search spaces from 200 SoS as earlier searched to a narrow band. The usage of GPU processing in image reconstruction and autofocusing further improves the time footprint of the calibration step.

3. EXPERIMENTAL RESULTS

A 256 element MSOT system was used for the experiments, as described by Razansky et. al. The laser source is an optical parametric oscillator (OPO) laser with 10 Hz pulse repetition and a tunable optical wavelength that was set to 720 nm in the experiments. The output laser beam was shaped to attain ring-type uniform illumination on the surface of the imaged object. An array of 256 cylindrically-focused array of immersion PZT transducers with a central frequency of 5 MHz and a focal length of 40 mm was employed to collect the optoacoustic signals, which were amplified and digitalized with a custom-made data acquisition system. The detector array offers 270 degree angular coverage in a given slice of focus. Each of the signals was averaged 10 times and band-pass filtered with cut-off frequencies between 0.4 and 7 MHz. The images were reconstructed with different values of SoS between 1460m/s to 1600m/s using GPU enhanced backprojection algorithms, and thereafter focus measures values were calculated. In figure 2 we illustrate the focus measures applied for calibration of SoS towards in-vivo mouse imaging results for the head (a), liver (b) and kidney/spleen(c) regions respectively. The calibrated SoS (most focused image) is denoted by the global minima (lowest point of the trough) of the curve. It is observed that the brain images show higher variability in the calibration graphs, primarily due to the lack of well-defined structures and edges to focus on. The algorithms are more robust and deterministic for the other part (regions b and c) of the mouse anatomy.

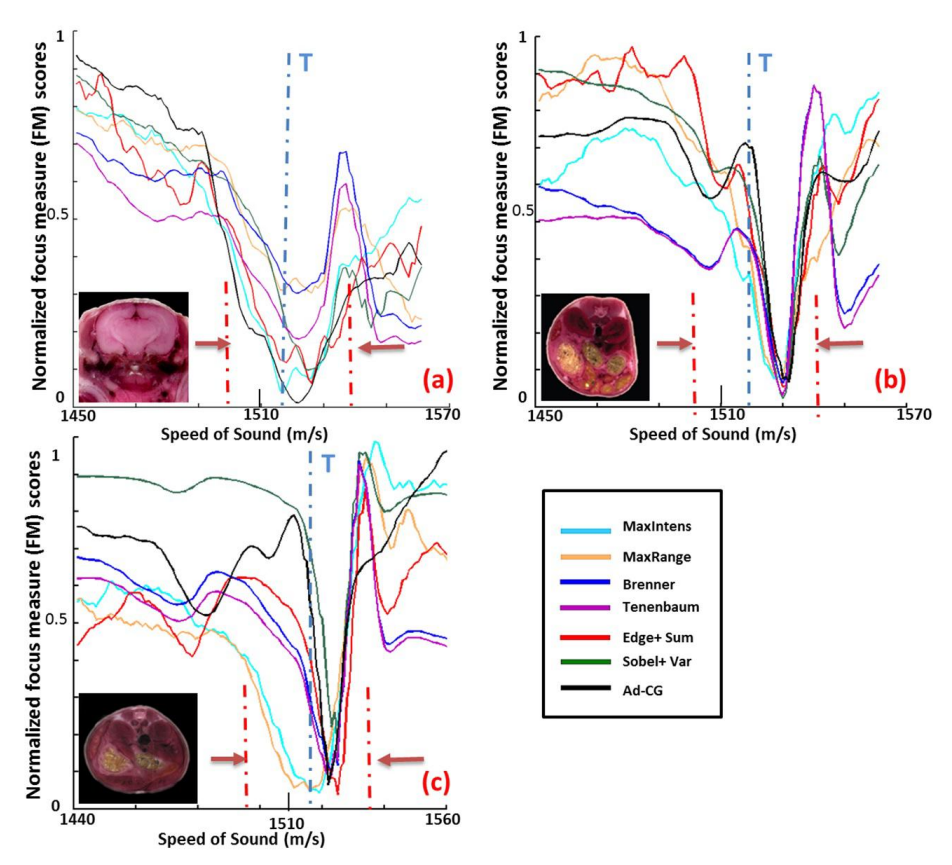


Figure 2: Performances of the focusing metrices in three different representative anatomical regions of mice head (a), liver (b) and kidney/spleen(c) are demonstrated [Windowed SOS prior: $(1510 \text{ m/s} \pm 25 \text{m/s})$ Temperature $= 33.9^{\circ}\text{C}$], cryosliced images of the referred anatomies are included for each region.

The temperature of the coupling medium (water) is used for referencing the SoS and reconstructing the data, as shown in Fig3 (marked by T). However, the manually fitted SoS (second column, marked with M), demonstrates that considering the SoS of the medium is not optimal, as the imaged tissue can have variations of up to 10% with respect to the SoS in water. The computational time of back-projection for generating a stack of 100 images at different SoS (200 x 200 pixels) are approximately 8.818 s, and for a windowed 50 SoS is

5.321s. Thus, we have an effective gain in efficiency by introducing the prior. A workstation with Intel i7-480 CPU operating at 3.70 GHz and with 32 GB of RAM was used for the experimentation. The back-projection reconstruction is further accelerated using the OpenGL platform on an AMD Raedeon GPU (Clock speed- 1100 MHz, Memory size 3072 MB, Shaders 2048).

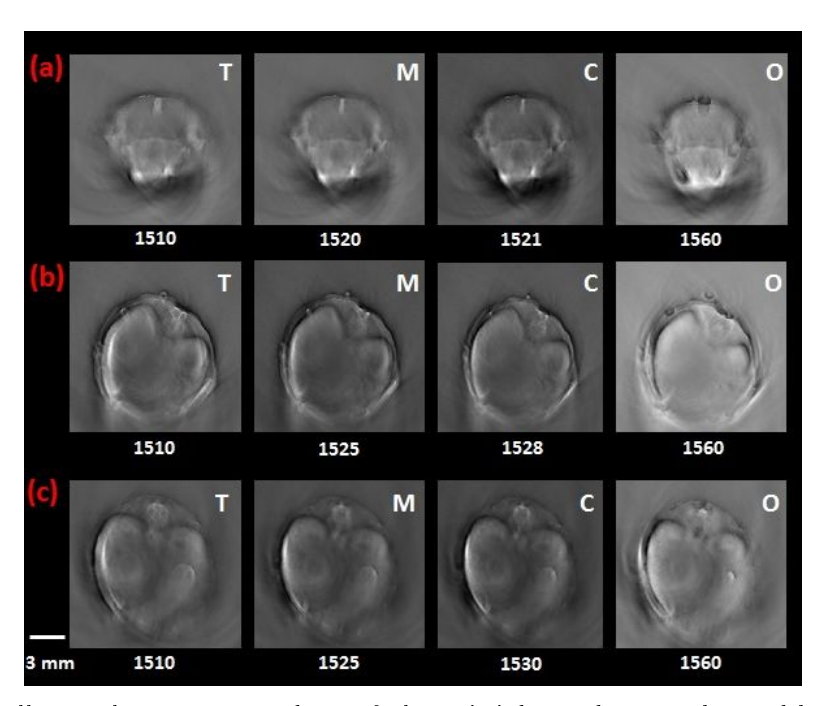


Figure 3: In vivo small animal imaging in and out of plane: 'T' denoted image obtained by applying SoS of the coupling medium as a reference, 'M' is the manually calibrated image and 'C' is the calibrated SoS using the focusing matrices. A constant uniform temperature and a single SoS is assumed for medium and the imaged object. Column 'O' shows images reconstructed with an erroneous SoS (2% error) for comparison.

4. CONCLUSIONS

In this article we have demonstrated the applicability of focusing techniques for automatic calibration of a uniform speed of sound value in optoacoustic tomographic reconstructions. The advanced methodologies presented integrated key image processing techniques to achieve better calibration performance for *in vivo* small animal images. Further, we used the temperature of the coupling medium to effectively reduce the computational cost and time complexity of the method. It can also be observed that the focusing techniques can be applied to calibration of other reconstruction parameters, as also for slice selections when large datasets are being investigated. Finally, it is worth mentioning that the method needs to be used with caution when the variation of SoS between the medium and the scanned object is very high (unlike soft tissues) or they have a huge divergence in temperature. Thus, several challenges and opportunities exist in the application of intelligent image processing techniques for improvement of reconstruction parameter evaluation, and their acceleration given a-priori information of the imaged object and coupling medium.

ACKNOWLEDGMENTS

Subhamoy Mandal acknowledges support (PhD Scholarship Award: A/11/75907) from the German Academic Exchange Service (DAAD). Daniel Razansky acknowledges support from the German Research Foundation (DFG) Research Grant (RA 1848/1) and the ERC Starting Independent Researcher Grant. H Garud (IIT Kharagpur) and N C Burton(iThera Medical GmbH) are acknowledged for their support in algorithm development and small animal imaging.

REFERENCES

- [1] Razansky, D., "Multispectral optoacoustic tomography volumetric color hearing in real time," Selected Topics in Quantum Electronics, IEEE Journal of 18(3), 1234–1243 (2012).
- [2] Razansky, D., Distel, M., Vinegoni, C., Ma, R., Perrimon, N., Köster, R. W., and Ntziachristos, V., "Multispectral opto-acoustic tomography of deep-seated fluorescent proteins in vivo," *Nature Photonics* 3(7), 412–417 (2009).
- [3] Razansky, D., Buehler, A., and Ntziachristos, V., "Volumetric real-time multispectral optoacoustic tomography of biomarkers," *Nature protocols* **6**(8), 1121–1129 (2011).
- [4] Van de Sompel, D., Sasportas, L. S., Dragulescu-Andrasi, A., Bohndiek, S., and Gambhir, S. S., "Improving image quality by accounting for changes in water temperature during a photoacoustic tomography scan," *PLoS ONE* 7, e45337 (10 2012).
- [5] Mandal, S., Deán-Ben, X. L., and Razansky, D., "Automated calibration of temporal changes in the speed of sound in optoacoustic tomography," *Proc. SPIE* 8800, 88000K–88000K–5 (2013).
- [6] Deán-Ben, X. L., Ntziachristos, V., and Razansky, D., "Effects of small variations of speed of sound in optoacoustic tomographic imaging.," *Medical physics* 41, 073301 (July 2014).
- [7] Mandal, S., Nasonova, E., Deán-Ben, X. L., and Razansky, D., "Optimal self-calibration of tomographic reconstruction parameters in whole-body small animal optoacoustic imaging," *Photoacoustics* 2(3), 128 136 (2014).
- [8] Paltauf, G., Viator, J. A., Prahl, S. A., and Jacques, S. L., "Iterative reconstruction algorithm for optoa-coustic imaging," *Journal of the Acoustical Society of America* 112(4), 1536–1544 (2002).
- [9] Norton, S. J. and Vo-Dinh, T., "Optoacoustic diffraction tomography: analysis of algorithms," *Journal of the Optical Society of America A* **20**(10), 1859–1866 (2003).
- [10] Deán-Ben, X. L., Buehler, A., Ntziachristos, V., and Razansky, D., "Accurate model-based reconstruction algorithm for three-dimensional optoacoustic tomography," *IEEE Transactions on Medical Imaging* 31(10), 1922–1928 (2012).
- [11] Filbir, F., Hielscher, R., and Madych, W. R., "Reconstruction from circular and spherical mean data," *Applied and Computational Harmonic Analysis* **29**(1), 111–120 (2010).
- [12] Lutzweiler, C., Deán-Ben, X. L., and Razansky, D., "Expediting model-based optoacoustic reconstructions with tomographic symmetries," *Medical physics* 41(1), 013302 (2014).
- [13] Treeby, B. E., Varslot, T. K., Zhang, E. Z., Laufer, J. G., and Beard, P. C., "Automatic sound speed selection in photoacoustic image reconstruction using an autofocus approach," *Journal of Biomedical Optics* **16**(9), 090501–090501–3 (2011).
- [14] Garud, H., Ray, A., Mandal, S., Sheet, D., Mahadevappa, M., and Chatterjee, J., "Volume visualization approach for depth-of-field extension in digital pathology," in [Image and Signal Processing (CISP), 2011 4th International Congress on], 1, 335–339 (2011).
- [15] Gonzalez, R. C., [Digital image processing], Pearson Education India (2009).
- [16] Groen, F. C., Young, I. T., and Ligthart, G., "A comparison of different focus functions for use in autofocus algorithms," *Cytometry* **6**(2), 81–91 (1985).
- [17] Perona, P. and Malik, J., "Scale-space and edge detection using anisotropic diffusion," *Pattern Analysis and Machine Intelligence, IEEE Transactions on* **12**(7), 629–639 (1990).
- [18] Ando, S., "Consistent gradient operators," Pattern Analysis and Machine Intelligence, IEEE Transactions on 22(3), 252–265 (2000).